ARTICLES

^{90}Y and ^{111}In Complexes of a DOTA-Conjugated Integrin $\alpha_v\beta_3$ Receptor Antagonist: Different but Biologically Equivalent

David C. Onthank, Shuang Liu,* Paula J. Silva, John A. Barrett,† Thomas D. Harris, Simon P. Robinson, and D. Scott Edwards

Discovery R & D, Bristol-Myers Squibb Medical Imaging, 331 Treble Cove Road, North Billerica, Massachusetts 01862. Received June 26, 2003; Revised Manuscript Received December 15, 2003

^{90}Y-TA138 is a ^{90}Y-labeled nonpeptide integrin $\alpha_v\beta_3$ receptor antagonist that binds with high affinity and specificity to integrin $\alpha_v\beta_3$ receptors overexpressed on both endothelial and tumor cells. ^{90}Y-TA138 has demonstrated significant therapeutic effects in several preclinical tumor-bearing animal models. Since ^{90}Y is a pure β-emitter, ^{111}In-TA138 has been chosen as the imaging surrogate for dosimetry determination of ^{90}Y-TA138. This report describes the synthesis of ^{111}In-TA138 and biological evaluations of both ^{111}In-TA138 and ^{90}Y-TA138 in the c-neu Oncomouse model. The HPLC data shows that ^{111}In-TA138 is more hydrophilic with the retention time ~4.5 min shorter than that of ^{90}Y-TA138 under identical chromatographic conditions. Since the only difference between ^{111}In-TA138 and ^{90}Y-TA138 is the metal ion, the HPLC retention time difference strongly suggests that indium and yttrium chelates do not share the same coordination sphere in solution even though they are coordinated by the same DOTA conjugate. Despite their differences in lipophilicity and solution structure, biodistribution data in the c-neu Oncomouse model clearly showed that ^{111}In-TA138 and ^{90}Y-TA138 are biologically equivalent with respect to their uptake in tumors and other major organs. Therefore, ^{111}In-TA138 is useful as an imaging surrogate for ^{90}Y-TA138 and should be able to predict the radiation dosimetry of ^{90}Y-TA138, a therapeutic radiopharmaceutical for treatment of rapidly growing tumors.

INTRODUCTION

There is currently a considerable interest in radiolabeled biomolecules (BM) as target-specific radiopharmaceuticals for diagnosis and treatment of cancers (*1*–*10*). DOTA and its analogues have been used as bifunctional chelators (BFCs) for the radiolabeling of a variety of biomolecules, including antibodies (*11*–*17*) and small peptides (*18*–*24*). While ^{90}Y-labeled DOTA–BM conjugates are used for tumor radiotherapy, ^{111}In-labeled DOTA–BM conjugates are often used as imaging surrogates for the purpose of dosimetry determination. This is largely based on the assumption that ^{90}Y- and ^{111}In-labeled DOTA–BM conjugates are chemically and biologically equivalent. However, results from recent literature have shown differences in biological properties between ^{90}Y- and ^{111}In-labeled BFC–BM conjugates (*25*–*27*). This causes some concerns about the validity of using ^{111}In-labeled BFC–BM conjugates as imaging surrogates for their ^{90}Y analogues.

We have been interested in developing diagnostic and therapeutic radiopharmaceuticals based on radiolabeled integrin $\alpha_v\beta_3$ receptor antagonists (*23*, *24*, *28*–*33*). In our previous communication (*32*), we reported synthesis of the ^{90}Y complex of a DOTA-conjugated nonpeptide integrin $\alpha_v\beta_3$ receptor antagonist (Figure 1: TA138). ^{90}Y-TA138 has been evaluated as a therapeutic radiopharmaceutical in preclinical tumor-bearing animal models (e.g. c-neu Oncomouse, HCT116, and HT460 xenografts). In all cases, tumor growth was significantly inhibited in mice treated with ^{90}Y-TA138 (30 mCi/kg) on day 7 and 11 after subcutaneous implantation of tumor cells in mice (*33*). As a continuation of these studies, we now present the synthesis of ^{111}In-TA138. To demonstrate the validity of ^{111}In-TA138 as the imaging surrogate for ^{90}Y-TA138, we have evaluated biodistribution characteristics of ^{111}In-TA138 and ^{90}Y-TA138 in the same c-neu Oncomouse model. Results from this study clearly demonstrated that ^{111}In-TA138 and ^{90}Y-TA138 are biologically equivalent with respect to their uptake in tumors and other major organs despite their differences in lipophilicity and solution structures.

EXPERIMENTAL SECTION

Materials. Ammonium acetate, diethylenetriaminepentaacetic acid (DTPA), and sodium gentisate were purchased from Sigma-Aldrich (St. Louis, MO) and were used as received. $^{90}YCl_3$ and $^{111}InCl_3$ (in 0.05 N HCl) were purchased from Perkin-Elmer Life Sciences, North Billerica, MA. Synthesis of TA138 (3-sulfon-*N*-[[4,7,10-tris(carboxymethyl)-1,4,7,10-tetraaza-cyclododec-1-yl]-acetyl]-L-alanyl-*N*-[2-[4-[[[(1*S*)-1-carboxy-2[[[1,4-dihydro-7-[(1*H*-imidazol-2-ylamino]methyl]-1-methyl-4-oxo-3-quinolinyl]carbonyl]amino]ethyl]amino]sulfonyl]-3,5-

* To whom correspondence should be addressed. Current address: Department of Industrial and Physical Pharmacy, School of Pharmacy, Purdue University, 575 Stadium Drive, West Lafayette, IN 47907-2051. Phone: 765-494-0236 (S. L.); Fax 765-496-3367; E-mail: lius@pharmacy.purdue.edu.

† Current address: EPIX Medical Inc., 71 Rogers St., Cambridge, MA 02142-1118.

10.1021/bc034108q CCC: $27.50
Published on Web 02/17/2004

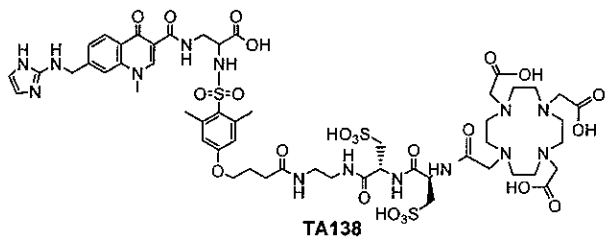

Figure 1. Structure of the DOTA-conjugated integrin $\alpha_v\beta_3$ receptor antagonist TA138.

dimethylphenoxy]-1-oxobutyl]amino]ethyl]-3-sulfo-L-alaninamide) has been described in our previous communication (*32*).

Analytical Methods. The radio-HPLC method used a HP-1100 HPLC system with an UV/visible detector (λ = 230 nm), an IN–US radio-detector, and a Zorbax C_{18} column (4.6 mm × 250 mm, 80 Å pore size). The flow rate was 1 mL/min with a gradient mobile phase starting from 92% solvent A (25 mM ammonium acetate buffer, pH 6.8) and 8% solvent B (acetonitrile) to 90% solvent A and 10% solvent B at 18 min. The mobile phase was isocratic using 40% of solvent A and 60% solvent B from 19 to 25 min. The TLC method used the C_{18} reverse phase glass plates and a mobile phase containing methanol, acetone, and saline (2:1:1 = v:v:v). By this method, both ^{90}Y-TA138 and ^{111}In-TA138 migrate to the solvent front while unchelated radiometal remains at the origin. The corrected radiochemical purity was calculated by subtracting the percentage of unchelated radiometal obtained by TLC from that obtained by radio-HPLC.

Synthesis of ^{90}Y-TA138. To a clean 10 mL vial containing 775 μg of TA138 were added 15.2 mg sodium gentisate and 7.6 mL of ammonium acetate buffer (0.5 M, pH = 6.0). The solution was immediately degassed under vacuum (<1.0 mmHg) for ~2 min. Upon addition of 175 μL of $^{90}YCl_3$ (~150 mCi) in 0.05 N HCl, the reaction mixture was heated at 95 °C for 5 min. After radiolabeling, a sample of the resulting solution was first diluted 40-fold with the 1.0 mM DTPA solution containing sodium gentisate (10 mg/mL) and was then analyzed by radio-HPLC and TLC. The radiochemical purity was 99.0% for ^{90}Y-TA138. The dose for animal studies was made by diluting part of the kit formulation to a concentration of ~50 μCi/mL with saline.

Synthesis of ^{111}In-TA138. TA138 (100 μg) and sodium gentisate (1.0 mg) were dissolved in 1.5 mL of ammonium acetate buffer (0.5 M, pH = 6.0). The resulting solution was immediately degassed under vacuum (<1 mmHg) for ~2 min. Upon addition of $^{111}InCl_3$ solution (2.2 mCi) in 0.05 N HCl, the reaction mixture was heated at 100 °C for 5 min. After cooling to room temperature, a sample of the resulting solution was analyzed by radio-HPLC and TLC. The radiochemical purity was 99.5% for ^{111}In-TA138. The dose for animal studies was made by diluting the solution above to a concentration of ~15 μCi/mL with saline.

In Vivo Biodistribution Study. The c-neu Oncomouse is a spontaneous tumor-bearing model that carries an activated c-neu oncogene driven by a mouse mammary tumor virus (MMTV) promoter. Transgenic mice uniformly expressing the MMTV/c-neu gene develop mammary adenocarcinomas (4 to 8 months postpartum) that involve the entire epithelium in each gland. The mice used in this study were obtained through an in-house breeding program and were anesthetized intramuscularly with 0.1 mL of a ketamine/acepromazine mixture (1.8 mL saline, 1.0 mL ketamine, and 0.2 mL acepromazine) prior to dosing and tissue sampling. Equal volumes of ^{90}Y-TA138 (50 μCi/mL) and ^{111}In-TA138 (15 μCi/mL) solutions were mixed before injection. The final concentration was 25 μCi/mL for ^{90}Y-TA138 and 7.5 μCi/mL for ^{111}In-TA138. Doses (0.1 mL) were drawn into 0.5 mL insulin syringes for injection.

Eighteen mice (~25 g) were divided into three groups according to the biodistribution time (2, 24, and 48 h) postinjection. Each group had six mice, and each mouse was administered a mixture (0.1 mL) containing ^{90}Y-TA138 at a dose of 2.5 μCi/mouse and ^{111}In-TA138 at a dose of 0.75 μCi/mouse in a single tail vein injection. Biodistributions were performed at the assigned time points (2, 24, and 48 h). Blood, eye, muscle, liver, kidney, bile, spleen, heart, lung, urine, stomach, colon, uterus, bone marrow, bone, and tumors were sampled and assayed for radioactivity. Since the c-neu Oncomouse spontaneously develops tumors in the mammary glands, most mice have more than one tumor. To assess the amount of uptake in the tumors, each tumor was sampled and counted separately. Subsequently, the activity was averaged to obtain an overall representation of tumor uptake. All tissue samples and injected dose aliquots were dissolved in 1 mL of Solvable (Packard Instrument Co., Meriden, CT) and incubated overnight at 37 °C. Each sample was then counted for 15 min on a calibrated Cobra gamma counter (Packard, Instrument Co., Meriden, CT) with dual window settings for counting each isotope. Raw radioactivity data was corrected for background and tested for quantitation limits according to the literature method (*34*). Results are shown in Figures 3–6 and are reported as a percent of the injected dose per gram of the tissue (%ID/g).

Data Analysis. Comparison of ^{90}Y-TA138 and ^{111}In-TA138 tissue uptake was evaluated for bioequivalence based on the 2002 bioequivalence guidance document adopted by the FDA. Briefly, this method describes the estimation of the difference between the means of the logarithms of the data, calculation of the 90% confidence interval for the mean difference, and taking the anti-logs of the limits of the 90% confidence interval. The test compounds are considered bioequivalent if the 90% confidence interval for the ratio of the means is between 0.8 and 1.25. ^{90}Y-TA138 and ^{111}In-TA138 were administered concurrently enabling the ratios of the tissue uptake (%ID/g) to be determined using paired-data analyses. For those organs that only had a single time point available (blood, muscle, bile, bone marrow, and bone), the comparison used the %ID/g. For those organs that had more than one time point available, the comparison used the area under the %ID/g versus time curve (AUC). In the single time point analyses, the paired-difference, log(%ID/g ^{111}In-TA138) − log(%ID/g ^{90}Y-TA138), was calculated for each animal. The mean paired-difference and the 90% confidence limits for the mean were calculated and the antilogarithms obtained to provide the mean and 90% confidence limits for the ratio %ID/g (^{90}Y-TA138)/%ID/g (^{111}In-TA138). The antilog data was necessary in order to express the data on the original scale of measurement. AUCs were estimated using trapezoidal approximations for the multiple time point analyses. The paired-difference, log[AUC(^{90}Y-TA138)] − log[AUC(^{111}In-TA138)], was calculated for each animal. The mean paired-difference and the 90% confidence limits for the mean were calculated and the antilogarithms obtained to provide the mean and 90% confidence limits for the ratio AUC (^{90}Y-TA138)/(^{111}In-TA138).

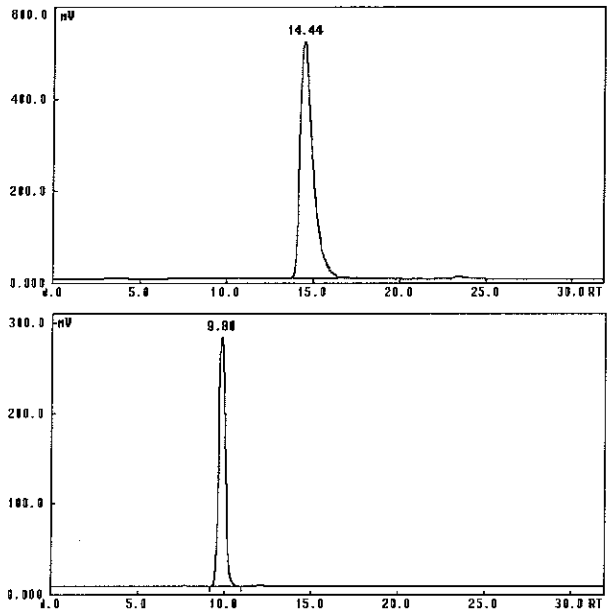

Figure 2. Radio-HPLC chromatograms of ^{90}Y-TA138 (top) and ^{111}In-TA138 (bottom) using a gradient mobile phase (8−10% B over 18 min, A = 25 mM ammonium acetate, B = acetonitrile).

RESULTS

Synthesis of ^{90}Y-TA138 and ^{111}In-TA138. ^{90}Y-TA138 was readily prepared in high yield (RCP > 98%) according to the procedure described in our previous communication (*32*). ^{111}In-TA138 was prepared using a similar procedure with slight modification. In both cases, exclusion of oxygen is required for successful radiolabeling and can be achieved either by degassing under vacuum or by bubbling nitrogen through the mixture before the addition of radiometal. Sodium gentisate was used as a radiolytic stabilizer to prevent radiolysis during the radiolabeling and HPLC analysis. In this study, we used ~100 μg of TA138 for 20 mCi of $^{90}YCl_3$ (TA138:^{90}Y ~170:1) for the synthesis of ^{90}Y-TA138, and 2.25 mCi of $^{111}InCl_3$ for preparation of ^{111}In-TA138. The corrected radiochemical purity for ^{90}Y-TA138 and ^{111}In-TA138 was >98% with minimal radiometal colloid formation.

HPLC Characterization of ^{90}Y-TA138 and ^{111}In-TA138. ^{90}Y-TA138 and ^{111}In-TA138 were analyzed by the same reversed phase HPLC method using a gradient mobile phase (8−10% B over 18 min, solvent A = 25 mM ammonium acetate buffer, solvent B = acetonitrile). Figure 2 shows typical radio-HPLC chromatograms of ^{90}Y-TA138 (top) and ^{111}In-TA138 (bottom). There are some small peaks (the void-volume peak at ~3.0 min and the wash-peak at ~23 min) due to radioimpurities in ^{90}Y-TA138 and ^{111}In-TA138 preparations. Since these radioimpurities are less than 1.0%, no further characterization was performed. The retention time of ^{111}In-TA138 is ~4.5 min shorter than that of ^{90}Y-TA138, suggesting that ^{90}Y-TA138 is more lipophilic than that of ^{111}In-TA138. We also tried other reversed phase HPLC methods. It was found that the HPLC retention time difference for ^{90}Y-TA138 and ^{111}In-TA138 depends on the gradient of the mobile phase. Under isocratic conditions (7% B over 30 min, solvent A = 25 mM ammonium acetate buffer, solvent B = acetonitrile), the HPLC retention time difference between ^{90}Y-TA138 and ^{111}In-TA138 was ~10 min.

Biodistributions of ^{90}Y-TA138 and ^{111}In-TA138 in the c-neu Oncomouse Model. ^{90}Y-TA138 and ^{111}In-TA138 showed rapid blood clearance (Figure 3) primarily via the renal system, and very similar biodistribution patterns (Figures 4−6) in the c-neu Oncomouse model over 48 h postinjection. At 2 h postinjection, the tumor uptake was ~10% ID/g for ^{90}Y-TA138 and ^{111}In-TA138. The uptake in the eye and bile were below the limit of quantification at 2 h postinjection. Activity levels of ^{90}Y-TA138 and ^{111}In-TA138 were also below the limit of quantification in the blood, muscle, bone, and bone marrow at 24 h postinjection while the uptake in other

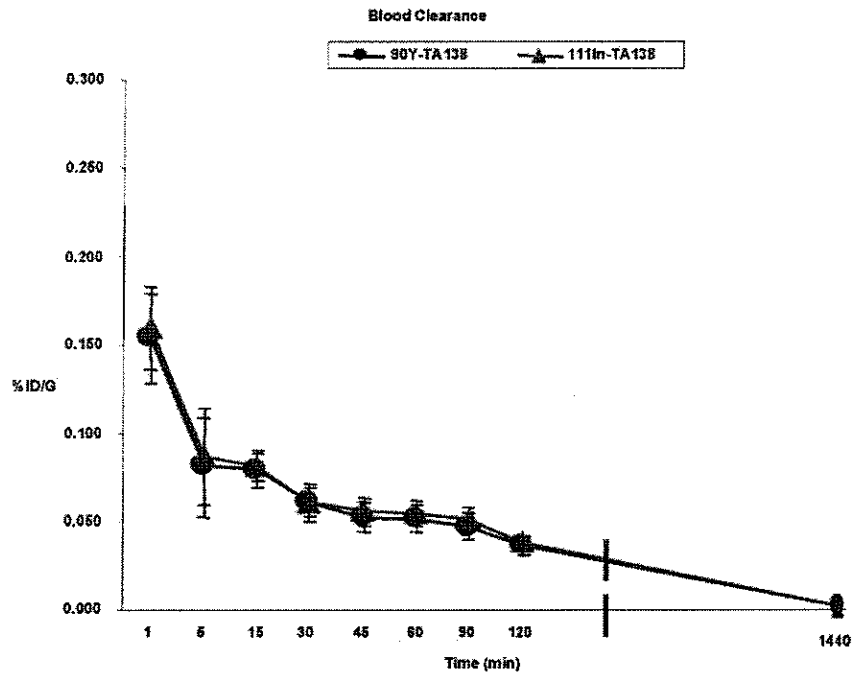

Figure 3. Blood clearance curve for ^{90}Y-TA138 and ^{111}In-TA138 in the c-neu Oncomouse model at 0−24 h postinjection. Each time point is the average ± the standard error of the mean (SEM) (n = 6).

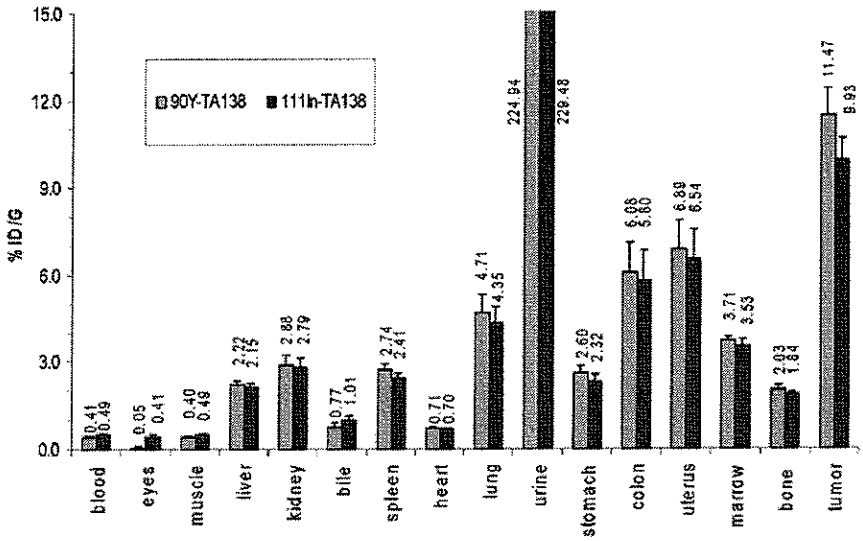

Figure 4. Biodistribution data for ^{90}Y-TA138 (left) and ^{111}In-TA138 (right) in the c-neu Oncomouse model at 2 h postinjection. Each histogram is the average ± the standard error of the mean (SEM) ($n = 6$). The data are decay corrected.

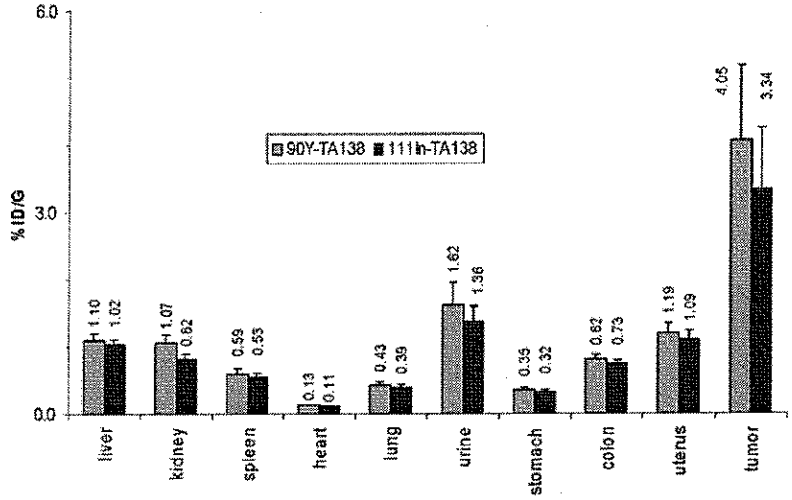

Figure 5. Biodistribution data for ^{90}Y-TA138 (left) and ^{111}In-TA138 (right) in the c-neu Oncomouse model at 24 h postinjection. Each histogram is the average ± the standard error of the mean (SEM) ($n = 6$). The data are decay corrected.

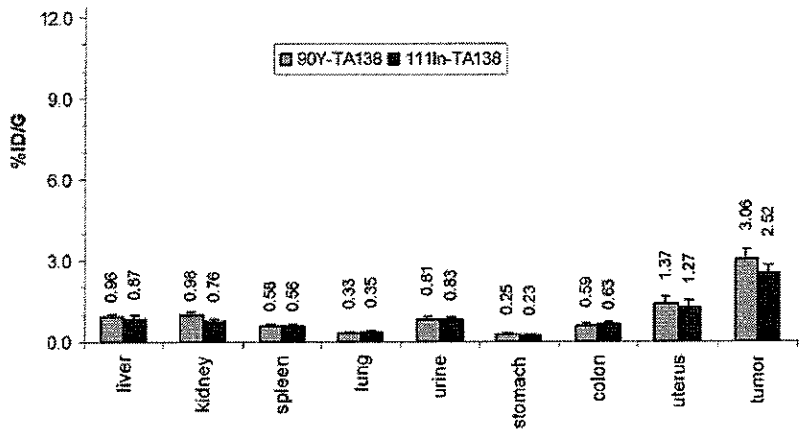

Figure 6. Biodistribution data for ^{90}Y-TA138 (left) and ^{111}In-TA138 (right) in the c-neu Oncomouse model at 48 h postinjection. Each histogram is the average ± the standard error of the mean (SEM) ($n = 6$). The data are decay corrected.

organs were less than 2% ID/g, except the tumor uptake of 3−4%ID/g. At 48 h postinjection, the uptake in all organs except tumor (2−3%) and uterus (1−2%) were less than 1% for ^{90}Y-TA138 and ^{111}In-TA138. At all the time points, there was no significant difference between ^{90}Y-TA138 and ^{111}In-TA138 with respect to their uptake in all organs of interest. HPLC analysis of blood and urine samples at 2 and 24 h postinjection showed no significant metabolism for both ^{90}Y-TA138 and ^{111}In-TA138.

DISCUSSION

^{90}Y-TA138 has demonstrated significant therapeutic effects in several preclinical tumor models, including c-Neu oncomouse, HCT116, and HT460 xenografts (*33*). Since ^{90}Y is a pure β-emitter, ^{111}In-TA138 was chosen as the imaging surrogate for biodistribution and dosimetry determination. Is ^{111}In-TA138 chemically and biologically equivalent to ^{90}Y-TA138? Can ^{111}In-TA138 be used to accurately predict the biodistribution and dosimetry of ^{90}Y-TA138 in animal models? With these questions in mind, we carried out the experiments described in this report.

Difference in Lipophilicity between ^{90}Y-TA138 and ^{111}In-TA138. Radio-HPLC has become a routine method for the characterization of radiolabeled compounds. It is also a powerful tool to compare lipophilicity of two closely related radiolabeled compounds. In this study, we used a reversed phase HPLC method with a gradient mobile phase. It was found that the retention time of ^{111}In-TA138 is ~4.5 min shorter than that of ^{90}Y-TA138 by the same HPLC method (Figure 2). Similar results were obtained for ^{90}Y and^{111}In complexes of DOTA-BA (BA = benzylamine), a model compound for DOTA−biomolecule conjugates (*35*). Since the only difference in ^{111}In-TA138 and ^{90}Y-TA138 is the metal ion, different retention times strongly suggest that indium and yttrium chelates do not share the same coordination sphere even though they are coordinated by the same DOTA conjugate. If indium and yttrium chelates were to share the same coordination sphere, ^{111}In-TA138 would have had the same retention time as that of ^{90}Y-TA138 under identical chromatographic conditions.

Structural Differences between Y and In Chelates in Solid State. Recently, Mäcke and co-workers (*18, 36*) described the crystal structures of complexes M(DOTA-D-Phe-NH_2) (M = Y and In) and found that both indium and yttrium in these complexes are eight-coordinated with four amine-nitrogen, one carbonyl-oxygen, and three carboxylate-oxygen atoms bonding to the metal center (*18, 36*). The difference between these two structures arises from the different conformation of ethylenic bridges and the orientation of sidearms. Y(DOTA-D-Phe-NH_2) exists in solid state as the m-isomer (traditionally designated as the minor isomer) while In(DOTA-D-Phe-NH_2) is observed as the M (major isomer) isomer. The same M isomer is also seen in In(DOTA-AA) (AA = *p*-aminoanilide) (*37*). Since the metal chelate is only one-third of the radiolabeled TA138, the slight difference in solid-state structures of yttrium and indium chelates hardly explains retention time differences between ^{90}Y-TA138 and ^{111}In-TA138 and is not consistent with solution dynamics of In(DOTA-BA) and In(DOTA-AA) as observed in our previous communication (*35, 37*).

Structural Differences between Y and In Chelates in Solution. The size of Y^{3+} (ionic radius = 0.87 Å) fits perfectly to the coordination cavity of the DOTA-monoamide chelator. It is not surprising that most yttrium complexes of DOTA derivatives are able to maintain their rigid eight-coordinated structure in solution (*18, 35, 38−41*). In^{3+} has an ionic radius of 0.75 Å, which is smaller than that of Y^{3+} (*42*). As a result, the coordination number for In^{3+} is typically 6 or 7 (*43−46*). Only a few eight-coordinated In^{3+} complexes are known (*36, 37, 47−49*). Due to its smaller size, In^{3+} does not fit to the coordination cavity of the DOTA-monoamide chelator. Although In^{3+} is eight-coordinated in the solid state of In(DOTA-monoamide), the carbonyl-oxygen may become dissociated in solution. This is particularly true for ^{111}In-TA138 at the tracer level (10^{-9} to 10^{-8} M). This explanation is consistent with the HPLC retention time differences between ^{90}Y-TA138 and ^{111}In-TA138, and the fluxionality of In(DOTA-BA) and In(DOTA-AA) in solution (*35, 37*).

Bioequivalence between ^{90}Y-TA138 and ^{111}In-TA138. There are several factors influencing the bioequivalence of ^{90}Y-TA138 and ^{111}In-TA138. These include solution structures and dissociation kinetics of radiometal chelates, specific activity of radiometals, and the amount of unlabeled TA138 injected into each animal. Since DOTA and its derivatives form eight-coordinated In(III) and Y(III) chelates with extremely high thermodynamic stability and kinetic inertness (*18, 38−41*), the dissociation kinetics may not contribute to the difference, if there is any, in biological properties of ^{90}Y-TA138 and ^{111}In-TA138. In this study we chose to administer ^{90}Y-TA138 and ^{111}In-TA138 concurrently into each animal so that we can eliminate the effect of specific activity and amount of unlabeled TA138 on biodistribution properties of ^{90}Y-TA138 and ^{111}In-TA138. In this way, the only remaining factor that can influence biodistribution properties of ^{90}Y-TA138 and ^{111}In-TA138 would be their structural differences between ^{90}Y and ^{111}In chelates in solution.

In the c-neu Oncomouse model, ^{90}Y-TA138 and ^{111}In-TA138 showed almost identical biodistribution patterns (Figures 4−6) over 48 h. Both ^{90}Y-TA138 and ^{111}In-TA138 are excreted rapidly from blood circulation (Figure 3) via the renal system. There was no significant difference between ^{90}Y-TA138 and ^{111}In-TA138 with respect to their uptake in tumor and other major organs of interest over 48 h postinjection. These results clearly demonstrated that ^{111}In-TA138 and ^{90}Y-TA138 are biologically equivalent despite their differences in solution structure and lipophilicity.

CONCLUSION

This report describes the synthesis and HPLC characterization of ^{111}In-TA138. The HPLC data showed that ^{111}In-TA138 is more hydrophilic, with the retention time being ~4.5 min shorter than that ^{90}Y-TA138. Since the only difference between ^{111}In-TA138 and ^{90}Y-TA138 is the metal ion, the HPLC retention time difference strongly suggests that indium and yttrium chelates do not share the same coordination sphere in solution even though they are coordinated by the same DOTA conjugate. Despite their differences in lipophilicity and solution structure, biodistribution data in the c-neu Oncomouse model clearly demonstrated that ^{111}In-TA138 and ^{90}Y-TA138 are biologically equivalent with respect to their uptake in tumors and other major organs. Therefore, ^{111}In-TA138 is useful as an imaging surrogate for ^{90}Y-TA138 and should be able to accurately predict the radiation dosimetry of ^{90}Y-TA138, which has the potential as a new therapeutic radiopharmaceutical for the treatment of rapidly growing solid tumors.

LITERATURE CITED

(1) Reubi, J. C. (1997) Regulatory peptide receptors as molecular targets for cancer diagnosis and therapy. *Quart. J. Nucl. Med. 41*, 63−70.

(2) Volkert, W. A. and Hoffman, T. J. (1999) Therapeutic radiopharmaceuticals. *Chem. Rev. 99*, 2269−2292.

(3) Kwekkeboom, D., Krenning, E. P., and de Jong, M. (2000) Peptide receptor imaging and therapy. *J. Nucl. Med. 41*, 1704−1713.

(4) Boerman, O. C., Oyen, W. J. G., and Corstens, F. H. M. (2000) Radiol-labeled receptor-binding peptides: A new class of radiopharmaceuticals. *Semin. Nucl. Med. 30*, 195−208.

(5) Liu, S., and Edwards, D. S. (2001) Bifunctional chelators for target specific therapeutic lanthanide radiopharmaceuticals. *Bioconjugate Chem. 12*, 7−34.

(6) Signore, A., Annovazzi, A., Chianelli, M., Coretti, F., Van de Wiele, C., Watherhouse, R. N., and Scopinaro, F. (2001) Peptide radiopharmaceuticals for diagnosis and therapy. *Eur. J. Nucl. Med. 28*, 1555−1565.

(7) Liu, S., and Edwards, D. S. (2002) Fundamentals of receptor-based diagnostic metalloradiopharmaceuticals. *Topics Curr. Chem. 222*, 259−278.

(8) Jong, M., Kwekkeboom, D., Valkema, R., and Krenning, E. P. (2003) Radiolabeled Peptides for tumor therapy: current status and future directions. *Eur. J. Nucl. Med. 30*, 463−469.

(9) Fichna, J., and Janecka, A. (2003) Synthesis of target-specific radiolabeled peptides for diagnostic imaging. *Bioconjugate Chem. 14*, 3−17.

(10) Liu, S., Robinson, S. P., and Edwards, D. S. (2003) Integrin $\alpha_v\beta_3$ directed radiopharmaceuticals for tumor imaging. *Drugs Future 28*, 551−564.

(11) Moi, M. K., Meares, C. F., McCall, M. J., Cole, W. C., and DeNardo, S. J. (1985) Copper chelates as probes of biological systems: stable copper complexes with macrocyclic bifunctional chelating agent. *Anal. Chem. 148*, 249−253.

(12) Moi, M. K., and Meares, C. F. (1988) The peptide way to macrocyclic bifunctional chelating agents: synthesis of 2-(*p*-nitrobenzyl)-1,4,7,10-tetraazacyclododecane-N,N′N″,N‴-tetraacetic acid and study of its yttrium(III) complex. *J. Am. Chem. Soc. 110*, 6266−6267.

(13) Kline, S. J., Betebenner, D. A., and Johnson, D. K. (1991) Carboxymethyl-substituted bifunctional chelators: preparation of aryl isothionate derivatives of 3-(carboxymethyl)-3-azapentanedioic acid, 3, 12-bis(carboxymethyl)-6,9-dioxa-3,12-diazatetradecanedioic acid, and 1, 4,7,10-tetraazacyclododecane-N,N′N″,N‴-tetraacetic acid for use as protein labels. *Bioconjugate Chem. 2*, 26−31.

(14) Li, M., and Meares, C. F. (1993) Synthesis, metal chelate stability studies, and enzyme digestion of a peptide-linked DOTA derivative and its corresponding radiolabeled immunoconjugates. *Bioconjugate Chem. 4*, 275−283.

(15) Lewis, M. R., Raubitschek, A., and Shively, J. E. (1994) A facile, water soluble method for modification of proteins with DOTA. Use of elevated temperature and optimized pH to achieve high specific activity and high chelate stability in radiolabeled immunoconjugates. *Bioconjugate Chem. 5*, 565−576.

(16) Kulis, D. L., DeNardo, S. J., DeNardo, G. L., O'Donnell, R. T., and Meares, C. F. (1998) Optimized conditions for chelation of yittrium-90-DOTA immunoconjugates. *J. Nucl. Med. 39*, 2105−2110.

(17) Lewis, M. R., and Shively, J. E. (1998) Maleimidocycteine-amido-DOTA derivatives: New reagents for radiometal chelate conjugation to antibody sulfhydryl groups undergo pH-dependent cleavage reactions. *Bioconjugate Chem. 9*, 72−86.

(18) Heppler, A., Froidevaux, S., Mäcke, H. R., Jermann, E., Béhé, M., Powell, P., and Hennig, M. (1999) Radiometal-labeled macrocyclic chelator-derived somatostatin analogue with superb tumor-targeting properties and potential for receptor-mediated internal therapy. *Chem. Eur. J. 5*, 1974−1981.

(19) De Jong, M., Bakker, W. H., Bernard, B. F., Valkema, R., Kwekkeboom, D. J., Reubi, J.-C., Srinivasan, A., Schmidt, M., and Krenning, E. P. (1999) Internalization of radiolabelled [DTPA°]octreotide and [DOTA°, Tyr^3]octreotide: peptides for somatostatin receptor-targeted scintigraphy and radionuclide therapy. *J. Nucl. Med. 40*, 2081−2087.

(20) Reubi, J. C., Waser, B., Schaer, J. C., Laederach, U., Erion, J., Srinivasam, A., Schmidt, M. A., and Bugaj, J. E. (1998) Unsulfated DTPA- and DOTA-CCK analogs as specific high affinity ligands for CCK−B receptor-expressing human and rat tissues in vitro and in vivo. *Eur. J. Nucl. Med. 25*, 481−490.

(21) Behr, T. M., Jenner, N., Béhé, M., Angerstein, C., Gratz, S., Raue, F., and Becker, W. (1999) Radiolabeled peptides for targeting cholecystokinin-B-gastrin receptor-expressing tumors. *J. Nucl. Med. 40*, 1029−1040.

(22) Behr, T. M., Jenner, N., Béhé, M., Angerstein, C., Gratz, S., Raue, F., and Becker, W. (1999) Cholecystokinin-B-gastrin receptor binding peptides: preclinical development and evaluation of their diagnostic and therapeutic potential. *Clin. Cancer Res. 5*, 3124s−3138s.

(23) Liu, S., Cheung, E., Rajopadyhe, M., Ziegler, M. C., Edwards, D. S. (2001) ^{90}Y-and ^{177}Lu-labeling of a DOTA-conjugated vitronectin receptor antagonist for tumor therapy. *Bioconjugate Chem. 12*, 559−568.

(24) Liu, S., and Edwards, D. S. (2001) Stabilization of ^{90}Y-labeled DOTA-biomolecule conjugates using gentisic and ascorbic acid. *Bioconjugate Chem. 12*, 554−558.

(25) Carrasquillo, J. A., White, J. D., Paik, C. H., Raubitschek, A., Le N., Rotman, M., Brechbiel, M. W., Gansow, O. A., Top, L. E., Perentesis, P., Reynolds, J. C., Nelson, D. L., and Waldmann, T. A. (1999) Similarities and differences in ^{111}In- and ^{90}Y-labeled 1B4M-DTPA antiTac monoclonal antibody distribution. *J. Nucl. Med. 40*, 268−276.

(26) Canera, L., Kinuya, S., Garmestani, K., Brechbiel, M. W., Wu, C., Pai, L. H., McMurry, T. J., Gansow, O. A., Pastan, I., Paik, C. H., and Carrasquillo, J. A. (1994) Comparative biodistribution of indium- and yttrium-labeled B3 monoalonal antibody conjugated to either 2-(p-SCN−Bz)-6-methyl-DTPA (1B4M-DTPA) or 2-(p-SCN−Bz-)-1,4,7,10-tetraazacyclododecane tetraacetic acid (2B-DOTA). *Eur. J. Nucl. Med. 21*, 640−646.

(27) Rösch, F., Herzog, H., Stolz, B., Brockmann, J., Köhle, M., Mühlensiepen, H., Marbach, P., and Müller-Gärtner, H.-W. (1999) Uptake kinetics of the somatostatin receptor ligand [^{86}Y]DOTA-$_D$Phe^1-Tyr^3-octreotide ([^{86}Y]SMT487) using positron emission tomography in nonhuman primates and calculation of radiation doses of the ^{90}Y-labeled analogue. *Eur. J. Nucl. Med. 26*, 358−366.

(28) Liu, S., Edwards, D. S., Ziegler, M. C., Harris, A. R., Hemingway, S. J., and Barrett, J. A. (2001) ^{99m}Tc-Labeling of a hydrazinonictotinamide-conjugated vitronectin receptor antagonist. *Bioconjugate Chem. 12*, 624−629.

(29) Liu, S., Cheung, E., Rajopadyhe, M., Williams, N. E., Overoye, K. L. and Edwards, D. S. Isomerism and solution dynamics of ^{90}Y-labeled DTPA- biomolecule conjugates. *Bioconjugate Chem.* **2001**, *12*, 84−91.

(30) Liu, S., and Edwards, D. S. (2001) Synthesis and characterization of two ^{111}In labeled DTPA-peptide conjugates. *Bioconjugate Chem. 12*, 630−634.

(31) Janssen, M., Oyen, W. J. G., Massuger, L. F. A. G., Frielink, C., Dijkgraaf, I., Edwards, D. S., Rajopadyhe, M., Corsten, F. H. M., and Boerman, O. C. Tumor targeting with radiolabeled alpha(v)beta(3) integrin binding peptides in nude mouse model. *Cancer Res* **2002**, *62*, 6146−6151.

(32) Liu, S., Harris, T. D., Ellars, C., and Edwards, D. S. (2003) Anaerobic ^{90}Y- and ^{177}Lu-labeling of a DOTA-conjugated nonpeptide vitronectin receptor antagonist. *Bioconjugate Chem. 14*, 1030−1037.

(33) Harris, T. D., Kalogeropoulos, S., Nguyen, T., Liu, S., Bartis, J., Ellars, C. E., Edwards, D. S., Onthank, D., Yalamanchili, P., Robinson, S. P., Lazewatsky, J., and Barrett, J. A. (2003) Design, synthesis and evaluation of radiolabeled integrin $\alpha_v\beta_3$ antagonists for tumor imaging and radiotherapy. *Cancer Biother. Radiopharm. 18*, 627−641.

(34) Currie, L. A. (1968) Limits for qualitative detection and quantitative determination. *Anal. Chem. 40*, 586−593.

(35) Liu, S., Pietryka, J., Ellars, C. E., and Edwards, D. S. (2002) Comparison of yttrium and indium complexes of

DOTA-BA and DOTA-MBA: models for ^{90}Y- and ^{111}In-labeled DOTA-biomolecule conjugates. *Biocorjugate Chem. 13*, 902–913.

(36) Maeke, H., Scherer, G., Heppeler, A., and Henig, M. (2001) Is In-111 an ideal surrogate for Y-90? If not, why? *Eur. J. Nucl. Med. 28*, 967 (abstract no. OS-27).

(37) Liu, S., He, Z.-J., Hsieh, W.-Y., and Fanwick, P. E. (2003) Synthesis, characterization, and crystal structure of In(DOTA-AA) (AA = *p*-aminoanilide): a model compounds for ^{111}In-labeled DOTA-biomolecule conjugates. *Inorg. Chem. 42*, 559–568.

(38) Aime, S., Botta, M., and Ermodi, G. (1992) NMR study of solution structures and dynamics of lanthanide(III) complexes of DOTA. *Inorg. Chem. 31*, 4291–4299.

(39) Aime, S., Anelli, P. L., Botta, M., Fedeli, F., Ermondi, G., Grandi, M., Paoli, P., and Uggeri, F. (1992) Synthesis, characterization, and *1/T*1 NMRD profiles of gadolinium(III) complexes of monoamide derivatives of DOTA-like ligands. X-ray structure of the 10-[2-[[2-hydroxy-1-(hydroxymethyl)-ethyl]amino]-1-(phenylmethoxy)methyl]2-oxoethyl]-1,4,7,10-tetraazacyclododecane-1,4,7-triacetic acid-gadolinium(III) complex. *Inorg. Chem. 31*, 2422–2428.

(40) Aime, S., Botta, M., Ermondi, G., Terreno, E., Anelli, P. L., Dedeli, F., and Uggeri, F. (1996) Relaxometric, structural, and dynamic NMR studies of DOTA-like Ln(III) complexes (Ln = La, Gd, Ho, Yb) containing a *p*-nitrophenyl substituent. *Inorg. Chem. 35*, 2726–2736.

(41) Kumar, K., Chang, C. A., Francesconi, L. C., Dischino, D. D., Malley, M. F., Cougoutas, J. Z., and Tweedle, M. F. (1994) Synthesis, stability, and structure of gadolinium(III) and yttrium(III) macrocyclic poly(amino carboxylates). *Inorg. Chem. 33*, 3567–3575.

(42) Shannon, R. D. (1976) Revised effective ionic radii and systemic studies of interatomic distances in halides and chalogenides. *Acta Crystallogr. A32*, 751–767.

(43) Yang, L.-W., Liu, S., Wong, E., Rettig, S. J., and Orvig, C. (1995) Lanthanide complexes of potentially heptadentate (N_4O_3) schiff base and aminephenol ligands: influence of rigidity and preorganization of ligands on compound structure. *Inorg. Chem. 34*, 2164–2178.

(44) Liu, S., Wong, E., Rettig, S. J., and Orvig, C. (1993) Hexadentate N_3O_3 amine phenol ligands for group 13 Metal Ions: Evidence for intrastrand and interstrand hrdrogen bonds in polydentate amine phenols. *Inorg. Chem. 32*, 4268–4276.

(45) Liu, S., Wong, E., Karunaratne, V., Rettig, S. J., and Orvig, C. (1993) Highly flexible chelating ligands for group 13 metals. Design, synthesis and characterization of hexadentate (N_3O_3) tripodal amine phenol ligand complexes of aluminum, gallium and indium. *Inorg. Chem. 32*, 1756–1765.

(46) Liu, S., Rettig, S. J., and Orvig, C. (1992) Polydentate ligand chemistry of group 13 metals: Effects of the size and donor-selectivity of metal ions on structures and properties of aluminum, gallium and indium complexes with potentially heptadentate (N_4O_3) amine phenol ligands. *Inorg. Chem. 31*, 5400–5407.

(47) Riesen, A., Kaden, T. A., Ritter, W., and Mäcke, H. R. (1989) Synthesis and X-ray structural characterization of seven coordinate macrocyclic In^{3+} complexes with relavance to radiopharmaceutical applications. *J. Chem. Soc., Chem. Commun.* 460–462.

(48) Mäcke, H. R., Riesen, A., and Ritter, W. (1989) The molecular structure of indium-DTPA. *J. Nucl. Med. 30*, 1235–1239.

(49) Malyrick M. A., Ilyhin, A. B., and Petrosyans, S. P. (1994) Seven- and eight-coordinate complexes of indium(III) with nitrilotriacetic acid. *Main Group Metal Chem. 17*, 707–717.

BC034108Q